

## The Ligand Field of Phase-Coupled Ligators

A. CEULEMANS,\* M. DENDOOVEN, and L. G. VANQUICKENBORNE

Received March 21, 1984

More than 20 years ago, Orgel predicted that  $\pi$  conjugation in bidentate ligands such as bipyridyl and acetylacetonate should give rise to a pronounced and specific symmetry lowering of the ligand field. This effect, which will be referred to as the Orgel effect, vanishes if the bidentate bridge is saturated; it must be attributed to a definite phase relationship between the  $p\pi$  valence orbitals on the coordinating atoms. Orgel also noted that for such phase-coupled ligators the conventional ligand field treatment is unjustified. This implies that many chelated complexes, which are of great importance in modern coordination chemistry, cannot adequately be described by currently available ligand field parameterization schemes. The purpose of this paper is to extend the angular-overlap model (AOM) of the ligand field, so as to include the effect of phase-coupled ligator atoms. Starting from a simple example, it is shown how phase coupling causes a specific breakdown of the AOM additivity postulate. A coupling operator is defined, which corresponds to the nonadditive bidentate term. Subsequently, the expressions are generalized for the case of a nonsymmetrical bidentate at an arbitrary position on the coordination sphere. In principle all relevant parameters can experimentally be determined. Especially, magnetic measurements should prove very useful in this respect. In a final section several mono-, bis-, and tris-chelated complexes of potential interest are discussed.

### I. Introduction

Our understanding of bonding in transition-metal chemistry is intimately related to the concept of functional chemical groups. The angular-overlap model (AOM) represents an attempt to mold this qualitative thinking into an adequate formalism.<sup>1-5</sup> The global ligand field (LF) potential is decomposed as a sum of individual ligand potentials. The action of each ligand potential is described by specifying a limited set of semiempirical quantities, corresponding to the different metal-ligand binding modes; these semiempirical quantities constitute the fundamental AOM parameters  $\sigma$ ,  $\pi$ , ...

Assuming rotational symmetry around the metal-ligand axis, the interaction modes between a single ligand L and the d-electron orbitals on the metal can be described by three independent parameters  $e_{\lambda}^L$  ( $\lambda = \sigma, \pi, \delta$ ), where the mode label  $\lambda$  refers to the appropriate  $C_{\infty v}$  representation. In practical applications it is possible to limit oneself to the use of only two contracted parameters per ligand,  $\sigma^L = e_{\sigma}^L - e_{\delta}^L$  and  $\pi^L = e_{\pi}^L - e_{\delta}^L$ , serving as a basis for a two-dimensional ligand functionality series (sometimes referred to as the two-dimensional spectrochemical series<sup>1a</sup>).

At a later stage the model was refined to incorporate the effect of nonlinearly ligating molecular ligands.<sup>6</sup> Typically these are planar ligands characterized by an aromatic or olefinic  $\pi$ -electron cloud, consisting of  $p_z$  orbitals, where the  $z$  direction is perpendicular to the ligand plane in the local ligand frame. In consequence the metal-ligand rotational symmetry is lowered to  $C_{2v}$ , and the twofold degeneracies of  $\lambda \neq 0$  representations are split. The  $\pi$  parameter for linear ligation is thus replaced by two parameters,  $\pi_{\parallel}$  and  $\pi_{\perp}$ , corresponding to interactions of the  $p\pi$  orbitals, which are respectively parallel and perpendicular to the ligand molecular plane. One could equally well assign the appropriate directions with  $C_{2v}$  symmetry labels,  $b_1$  and  $b_2$ , since the parameter anisotropy in essence represents a symmetry factoring of the metal-ligand binding modes.

In plane  $\pi$  contributions are often considered negligible, so that ligands such as pyridine or mesityl are still described by two effective parameters,  $\sigma$  and  $\pi_{\perp}$ . Hence, nonlinear ligation not necessarily leads to an increase in the number of parameters, at

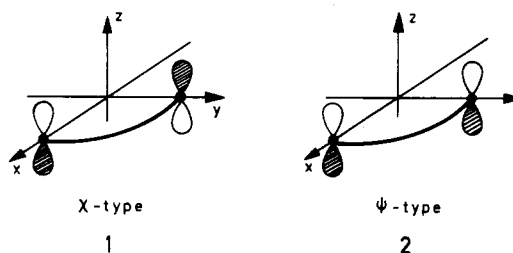
least if structural data regarding the orientation of the ligand plane are available.

A more specific and well-documented case of ligator symmetry lowering occurs in planar bidentate ligands, where  $\pi$  conjugation extends over both coordinating atoms. Quite remarkably, the effect was preconceived and explained by Orgel,<sup>7</sup> long before clear experimental indications were available. In recent times Orgel's original ideas have found substantial and unambiguous support from experiment. Yet, the conventional angular-overlap treatment is unable to account for the Orgel effect.

It is our purpose to examine why AOM is deficient in this respect and how it can be adapted in a formal way to account for the metal-ligand bonding in  $\pi$ -conjugated chelated complexes. Subsequently, the here developed formalism will be applied to several test cases. Review of a special class of applications, viz. low-spin Co(II) complexes involving Schiff-base ligands, will be deferred to a following paper.<sup>8</sup>

### II. The Model

**A. Symmetrical Bidentate Ligands.** First, consider the simplest case of a symmetrical bidentate ligand, with identical ligator atoms, and characterized by a bite angle of  $90^\circ$ . Following Orgel,<sup>7</sup> the frontier molecular orbital (MO) on the ligand can be classified with respect to a twofold rotation axis, bisecting the chelate angle; it is either symmetric, denoted  $\chi$ , or antisymmetric, denoted  $\psi$ . The  $p_z$  orbitals on the coordinating atoms are out of phase in the  $\chi$ -type MO (1) and in phase in the  $\psi$ -type MO (2). No other



role will be attributed to the remaining part of the bidentate bridge than to maintain the phase relationship of the outer orbitals. In 1 and 2 ligand positions are chosen on coordinate axes, which is the usual orientation for orthoaxial complexes. According to conventional AOM, refined for nonlinear coordination ( $\pi_{\parallel} \neq \pi_{\perp}$ ),  $p\pi$  interactions diagonalize the LF matrix describing the metal-bidentate interaction. The relevant part of this matrix is given in eq 1.

Clearly, in AOM  $|xz\rangle$  and  $|yz\rangle$  orbitals display a characteristic tetragonal degeneracy. Quite on the contrary the symmetry of

- (1) (a) McClure, D. S. *Proceedings of the Sixth International Conference on Coordination Chemistry*; Macmillan: New York, 1961; p 498. (b) Schäffer, C. E.; Jørgensen, C. K. *Mol. Phys.* **1965**, *9*, 401.  
 (2) Glerup, J.; Mønsted, O.; Schäffer, C. E. *Inorg. Chem.* **1976**, *15*, 1399.  
 (3) Jørgensen, C. K. "Modern Aspects of Ligand Field Theory"; North-Holland Publishing Co.: Amsterdam, 1971.  
 (4) Vanquickenborne, L. G.; Vranckx, J.; Görller-Walrand, C. *J. Am. Chem. Soc.* **1974**, *96*, 4121.  
 (5) (a) Vanquickenborne, L. G.; Ceulemans, A. *J. Am. Chem. Soc.* **1977**, *99*, 2208. (b) Vanquickenborne, L. G.; Ceulemans, A. *Inorg. Chem.* **1981**, *20*, 110. (c) Vanquickenborne, L. G.; Ceulemans, A. *Coord. Chem. Rev.* **1983**, *48*, 157.  
 (6) Schäffer, C. E. *Struct. Bonding (Berlin)* **1968**, *5*, 68.

(7) Orgel, L. E. *J. Chem. Soc.* **1961**, 3683.

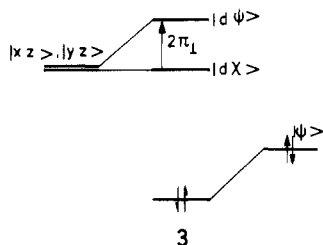
(8) Ceulemans, A.; Dendooven, M.; Vanquickenborne, L. G. *Inorg. Chem.* **1985**, *24*, 1159.

$$\mathcal{V}^{\text{AOM}} \begin{array}{l} \langle xz | \\ \langle yz | \\ \langle xy | \end{array} \begin{array}{l} |xz\rangle \\ |yz\rangle \\ |xy\rangle \end{array} = \begin{array}{l} \pi_{\perp} \quad 0 \quad 0 \\ 0 \quad \pi_{\perp} \quad 0 \\ 0 \quad 0 \quad 2\pi_{\parallel} \end{array} \quad (1)$$

the conjugated  $\pi$  functions is only  $C_{2v}$ .  $\psi$ - and  $\chi$ -type orbitals span different  $C_{2v}$  representations and the matching d-orbital combinations are respectively the in- and out-of-phase linear combinations of  $|xz\rangle$  and  $|yz\rangle$ , as given in eq 2a. Since only equi-

$$\begin{aligned} |d\psi\rangle &= (1/2^{1/2})(|xz\rangle + |yz\rangle) \\ |d\chi\rangle &= (1/2^{1/2})(|xz\rangle - |yz\rangle) \end{aligned} \quad (2a)$$

symmetric orbitals can interact, the actual chelate field will cause a significant splitting of the d orbitals. As an example, if the bidentate is a  $\pi$  donor with a  $\psi$ -type frontier orbital (3), the  $|d\chi\rangle$



orbital is not affected by the bidentate field, while the  $|d\psi\rangle$  combination is destabilized. We propose to parameterize the extent of the destabilization as  $2\pi_{\perp}$ , so that the barycenter energy remains equal to the AOM barycenter expression as in eq 1. The interaction matrix can now easily be deduced, working backwards from the solution in 3. The corresponding operator will be denoted  $\mathcal{V}(\psi)$  (see eq 3). The off-diagonal matrix elements in eq 3a do

$$\mathcal{V}(\psi) \begin{array}{l} \langle xz | \\ \langle yz | \end{array} \begin{array}{l} |xz\rangle \\ |yz\rangle \end{array} = \begin{array}{l} \pi_{\perp} \quad \pi_{\perp} \\ \pi_{\perp} \quad \pi_{\perp} \end{array} \quad (3a)$$

not correspond to any net stabilization or destabilization of the  $(xz, yz)$  set; they describe a pure splitting field caused by the phase coupling of the two bidentate ligands. The operator  $\mathcal{V}(\psi)$  represents the total perturbation, due to the conjugated  $\pi$  chain of the chelate ligand. The matrix elements involving  $|d_{xy}\rangle$  are identical with the corresponding matrix elements of  $\mathcal{V}^{\text{AOM}}$  in eq 1.

Similarly, if the frontier orbital is out-of-phase coupled, the  $|d\psi\rangle$  and  $|d\chi\rangle$  orbitals are interchanged and the following interaction matrix is obtained:

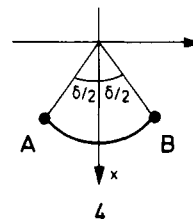
$$\mathcal{V}(\chi) \begin{array}{l} \langle xz | \\ \langle yz | \end{array} \begin{array}{l} |xz\rangle \\ |yz\rangle \end{array} = \begin{array}{l} \pi_{\perp} \quad -\pi_{\perp} \\ -\pi_{\perp} \quad \pi_{\perp} \end{array} \quad (4)$$

By comparison of the matrices in eq 1–4, the following observations can be made: (i) In all three cases only ligator atoms in the first coordination sphere are explicitly taken into account. The symmetry lowering in the bidentates is not obtained via weak interactions of bridging atoms in the second coordination shell. (ii) Phase decoupling can easily be achieved by taking the average of eq 3 and 4. This leads automatically to the AOM result, as expressed in the equation (5). As a matter of principle AOM

$$\mathcal{V}^{\text{AOM}} = 1/2(\mathcal{V}(\psi) + \mathcal{V}(\chi)) \quad (5)$$

ignores phase relationships, since they violate the basic postulate of ligand additivity. The symmetry lowering in the first coordination sphere of phase-coupled bidentates is thus in principle incompatible with the additive LF model. The Orgel effect can only be taken into account if a specific breakdown of ligand additivity is allowed for.

**B. Asymmetrical Bidentate Ligands.** We shall now attempt to generalize the previous description to the case of nonsymmetrical bidentates with a varying bite angle  $\delta$ . The bite angle can never deviate too far from  $\pi/2$ ;  $\delta = 0$  is an obviously absurd situation. In what follows, we will choose the standard ligand orientation as indicated in 4, where the bidentate plane coincides with the



cartesian  $xy$  plane and the  $x$  axis bisects the bite angle. A and B denote the two coordinating nuclei. Although this coordinate system may not seem the most obvious choice—especially with respect to the strong  $\sigma$  interactions—the ligand orientation in 4 proves to be particularly convenient in the description of the  $\pi$  interactions.

Reformulating the symmetrical  $\mathcal{V}(\psi)$  problem of the previous section in 4 leads to

$$|d\psi\rangle = |xz\rangle \quad |d\chi\rangle = |yz\rangle \quad (2b)$$

and therefore  $\langle\psi|d\chi\rangle = 0$ ; the rotated matrix becomes

$$\mathcal{V}(\psi) \begin{array}{l} \langle xz | \\ \langle yz | \end{array} \begin{array}{l} |xz\rangle \\ |yz\rangle \end{array} = \begin{array}{l} 2\pi_{\perp} \quad 0 \\ 0 \quad 0 \end{array} \quad (3b)$$

If  $A \neq B$ , no symmetry elements other than the coordinate plane are conserved and  $|xz\rangle$ ,  $|yz\rangle$ ,  $|\psi\rangle$  are equisymmetric; therefore, the matrix of the  $\pi_{\perp}$  interactions becomes slightly more complicated.

The diagonal matrix elements of  $\mathcal{V}(\psi)$  in the  $\{|xz\rangle, |yz\rangle\}$  basis can be evaluated by adopting the conventional AOM hypothesis, setting the d-orbital energies proportional to the square of the metal–ligand overlap integrals.<sup>3</sup> Hence

$$\langle xz | \mathcal{V}(\psi) | xz \rangle = k(\psi | xz)^2 \quad (6a)$$

$$\langle yz | \mathcal{V}(\psi) | yz \rangle = k(\psi | yz)^2 \quad (6b)$$

The proportionality constant  $k$  depends on the zero-order orbital energies of donor and acceptor levels. Since one and the same ligand orbital is involved in eq 6a,b, the same  $k$  can be used throughout. The off-diagonal element  $\langle xz | \mathcal{V}(\psi) | yz \rangle$  can also be obtained from the overlap criterion. Indeed, using a standard orthogonalization procedure, one easily finds a linear combination of the metal orbitals,  $|yz\rangle$  and  $|xz\rangle$ , that is orthogonal to the ligand orbital  $|\psi\rangle$ . The resulting combination reads

$$N[(\psi | xz) | yz \rangle - (\psi | yz) | xz \rangle] \quad (7)$$

where the normalization constant  $N = [(\psi | xz)^2 + (\psi | yz)^2]^{-1/2}$ . In the spirit of AOM this function will have zero energy since it does not show overlap with the ligand basis orbital. From this requirement and eq 6, the desired off-diagonal element immediately follows:

$$\langle xz | \mathcal{V}(\psi) | yz \rangle = k(\psi | xz)(\psi | yz) \quad (8)$$

The overlap integrals  $(\psi | xz)$  and  $(\psi | yz)$  can be expressed as a function of the angle  $\delta$  and of the value of the standard overlap integrals between the ligator-localized parts of the  $\psi$  orbital and a  $d\pi$  orbital, directed toward that particular ligator atom. If the absolute value of the latter integrals is denoted  $S_A$  and  $S_B$  for the ligators A and B, respectively, one readily obtains

$$(\psi | xz) = S_A \cos(\delta/2) + S_B \cos(\delta/2) \quad (9a)$$

$$(\psi | yz) = -S_A \sin(\delta/2) + S_B \sin(\delta/2) \quad (9b)$$

From the logic of AOM, fundamental  $\pi_{\perp}$  parameters can now be defined as in eq 10. Positive values of  $k$  (and thus of the  $\pi_{\perp}$

$$\pi_{\perp}^A = kS_A^2 \quad (10a)$$

$$\pi_{\perp}^B = kS_B^2 \quad (10b)$$

$$\pi_{\perp}^{AB} = kS_A S_B = \pm(\pi_{\perp}^A \pi_{\perp}^B)^{1/2} \quad (10c)$$

parameters) mark  $\pi$ -donor ligands, while negative  $k$  values correspond to  $\pi$ -acceptor ligands. The symbol  $\pi_{\perp}^{AB}$  is introduced

to denote the signed geometrical mean of  $\pi_{\perp}^A$  and  $\pi_{\perp}^B$ ; again, the sign parallels the donor or acceptor nature of the ligand orbital.

Combining these definitions with the expressions in eq 6 and 8 finally yields the standard interaction matrix for an unsymmetrical  $\psi$ -type bidentate ligand in the reference position, shown in 4:

$$\begin{array}{l} \mathcal{V}(\psi) \\ \langle xz | \\ \langle xz | \end{array} \begin{array}{l} |xz\rangle \\ (\pi_{\perp}^A + \pi_{\perp}^B + 2\pi_{\perp}^{AB}) \times \\ \cos^2(\delta/2) \end{array} \begin{array}{l} |yz\rangle \\ (\pi_{\perp}^B - \pi_{\perp}^A) \sin(\delta/2) \times \\ \cos(\delta/2) \end{array} \quad (11)$$

$$\begin{array}{l} \langle yz | \\ \langle yz | \end{array} \begin{array}{l} (\pi_{\perp}^B - \pi_{\perp}^A) \sin(\delta/2) \times \\ \cos(\delta/2) \end{array} \begin{array}{l} (\pi_{\perp}^A + \pi_{\perp}^B - 2\pi_{\perp}^{AB}) \times \\ \sin^2(\delta/2) \end{array}$$

The determinant of this matrix is zero, implying that one eigenvalue will be zero. The corresponding eigenfunction is of course the linear combination in eq 7, which shows no overlap with the ligand orbital  $|\psi\rangle$ . This eigenfunction will in general be denoted as  $|d\chi\rangle$ . Evidently, the orthogonal counterpart of  $|d\chi\rangle$  is a function that maximizes overlap with  $|\psi\rangle$  and therefore will be denoted as  $|d\psi\rangle$ , in agreement with the earlier notation in eq 2. This eigenvector carries the total destabilization due to the  $\mathcal{V}(\psi)$  field. Its energy therefore equals the sum of the diagonal elements in the interaction matrix.

$$\epsilon(d\chi) = 0 \quad (12a)$$

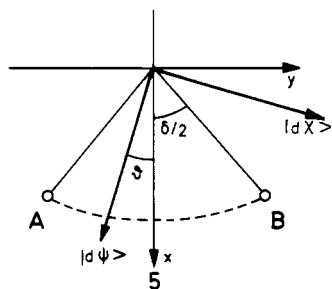
$$\epsilon(d\psi) = \pi_{\perp}^A + \pi_{\perp}^B + 2\pi_{\perp}^{AB} \cos \delta \quad (12b)$$

It is of interest to rewrite the nonoverlapping function and its orthogonal counterpart in a general trigonometric form:

$$|d\chi\rangle = \sin \theta |xz\rangle - \cos \theta |yz\rangle \quad (13a)$$

$$|d\psi\rangle = \cos \theta |xz\rangle + \sin \theta |yz\rangle \quad (13b)$$

These functions are seen to correspond to  $d_{qz}$ -type orbitals, where the  $q$  axis (situated in the  $xy$  plane) makes an angle of  $\theta$  with the bisector axis in the case of the  $|d\psi\rangle$  component. The  $q$  direction of  $|d\chi\rangle$  is of course perpendicular to the  $q$  direction of  $|d\psi\rangle$ , as shown in 5: the original orbital set  $\{|xz\rangle, |yz\rangle\}$  has simply been rotated over an angle  $\theta$  about the  $z$  axis.  $\theta$  will never deviate very far from zero and at any rate  $-\delta/2 \leq \theta \leq \delta/2$ .



The numerical value of  $\theta$  can be obtained from eq 7 and 13a:

$$\tan \theta = (\psi|yz\rangle) / (\psi|xz\rangle) \quad (14)$$

From eq 9, it is possible to express  $\theta$  as a function of  $S_A$ ,  $S_B$ , and  $\delta$  by

$$\tan \theta = \frac{S_B - S_A}{S_B + S_A} \tan \frac{\delta}{2} \quad (15)$$

or alternatively, from eq 10, as a function of the  $\pi_{\perp}$  parameters by

$$\tan \theta = \frac{\pi_{\perp}^B - \pi_{\perp}^A}{\pi_{\perp}^A + \pi_{\perp}^B + 2\pi_{\perp}^{AB}} \tan \frac{\delta}{2} \quad (16)$$

Several aspects of these solutions require further discussion.

(i) In a symmetrical bidentate, where  $\pi_{\perp}^A = \pi_{\perp}^B$ , the off-diagonal elements of eq 11 are zero and the  $|d\psi\rangle$  direction coincides with the bisector ( $\theta = 0$ ). In asymmetrical bidentates, the eigenvector is rotated toward the ligand with the larger  $\pi_{\perp}$  strength, as can be seen from eq 16. Therefore,  $\theta$  constitutes a direct

experimentally accessible measure of the degree of chelate asymmetrization.

(ii) In the interaction matrix of eq 11, one can distinguish terms depending on the separate parameters  $\pi_{\perp}^A$  and  $\pi_{\perp}^B$  vs. terms containing the combined  $\pi_{\perp}^{AB}$  parameter. First of all, it is well to stress that  $\pi_{\perp}^{AB}$  is not an independent new parameter: it is simply the geometric mean of the individual ligator parameters (as in the case of the symmetrical chelates). The terms depending on the individual  $\pi_{\perp}^A$  and  $\pi_{\perp}^B$  parameters simply correspond to the AOM interaction matrix for two separate and independent ligands A and B, positioned as in 4. At the operator level,  $\mathcal{V}(\psi)$  can therefore be represented as the sum

$$\mathcal{V}(\psi) = \mathcal{V}^{AOM} + \mathcal{V}^{cplng} \quad (17a)$$

where  $\mathcal{V}^{AOM}$  refers to the separate additive ligand field associated with ligand position 4 and  $\mathcal{V}^{cplng}$  represents the interligand terms, which are due to the specific phase coupling of the coordination orbitals.

From a completely analogous treatment, one finds for a  $\chi$ -type ligand orbital

$$\mathcal{V}(\chi) = \mathcal{V}^{AOM} - \mathcal{V}^{cplng} \quad (17b)$$

By combination of eq 17a and 17b the AOM potential reappears as the average of  $\mathcal{V}(\psi)$  and  $\mathcal{V}(\chi)$ , as already expressed in eq 5. This averaging precisely corresponds to the reinstallation of ligand additivity.

(iii) For asymmetrical chelates, the ligand  $\chi$  and  $\psi$  orbitals of course do not satisfy the original Orgel criterion of being symmetric or antisymmetric with respect to a twofold rotation axis. They are better referred to as in-phase ( $\psi$ -type) or out-of-phase ( $\chi$ -type) molecular orbitals on the ligands.

**C. Generalized Ligand Orientation.** Posed in its most general form, the bidentate problem involves the calculation of the interaction matrix for an asymmetrical bidentate at an arbitrary location on the coordination sphere. This location is completely specified by the pair of angular coordinates  $(\theta, \varphi)$  of both ligator atoms. There is little advantage in treating the bidentate moiety as one single superligand, since, except for  $\pi_{\perp}$  interactions, the additive ligand field of the separate ligator atoms apparently is preserved. We therefore adhere to the decomposition of the bidentate field in  $\mathcal{V}^{AOM}$  and  $\mathcal{V}^{cplng}$  (see eq 17) and construct separate rotation matrices for each potential.

The evaluation of the additive potential  $\mathcal{V}^{AOM}$  at arbitrary ligand positions creates no new problem, as it follows at once from the established AOM techniques. Hence, one specifies three AOM parameters per ligator atom ( $\sigma^A, \pi_{\parallel}^A, \pi_{\perp}^A, \sigma^B, \pi_{\parallel}^B, \pi_{\perp}^B$ ) and constructs the relevant AOM rotation matrices. Unlike the case of monodentate planar ligands, the orientation of the ligand plane is fixed by the bidentate bridge. Therefore, knowledge of the angular coordinates  $(\theta, \varphi)$  for the ligator atoms A and B immediately specifies the directions of the  $\pi_{\parallel}$  and  $\pi_{\perp}$  interactions of the chelate. Formally, this information can most readily be incorporated by introducing the third Euler angle, as shown in Figure 1. We will adopt the convention that a ligator atom, say A, is in the reference position ( $\theta = \varphi = \psi = 0$ ) if A is situated on the positive  $z$  axis while B (and therefore the chelate plane) is in the  $xz$  plane and, more specifically, at positive  $x$ . In Figure 1, the bidentate ligand with A in the reference position is denoted as  $A_0B_0$ . Clearly, in this position the AOM interaction matrix of ligand A will be diagonal, yielding the following eigenvalues:

$$\begin{array}{lll} \epsilon(d_{z^2}) = \sigma^A & \epsilon(d_{xz}) = \pi_{\parallel}^A & \epsilon(d_{yz}) = \pi_{\perp}^A \\ \epsilon(d_{xy}) = \epsilon(d_{x^2-y^2}) = 0 \end{array} \quad (18)$$

Hence, alternatively the parameters  $\pi_{\parallel}^A$  and  $\pi_{\perp}^A$  may also be denoted  $\pi_{xz}^A$  and  $\pi_{yz}^A$ , respectively, where  $xz$  and  $yz$  refer to the  $d$  orbital that is destabilized by the ligand field of A in the reference position. The motion of the chelate from this position to the standard situation in 4 can formally take place in three steps: first, the chelate is rotated about the  $z$  axis over an angle  $\psi_A$ , yielding  $A_1B_1$ ; subsequently,  $A_1B_1$  is rotated about the  $y$  axis over an angle  $\theta_A$  to yield  $A_2B_2$ ; finally,  $A_2B_2$  is rotated about the  $z$  axis

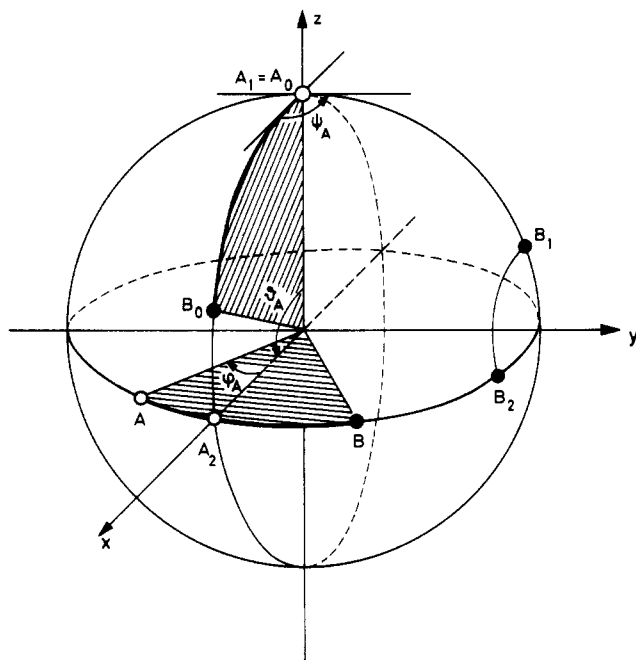


**Figure 1.** Set of the three Euler angles, characterizing the angular position ( $\theta_A, \varphi_A$ ) and chelate orientation ( $\psi_A$ ) of a ligator atom A that is part of a bidentate AB. The three angles refer to three consecutive rotations that carry the ligator atom from the reference position  $A_0B_0$  to an arbitrary position AB. First, the chelate plane is rotated about the z axis over an angle  $\psi_A$  ( $A_0B_0 \rightarrow A_1B_1$ ). Second, one rotates about the y axis over  $\theta_A$  ( $A_1B_1 \rightarrow A_2B_2$ ). The final rotation is again about the z axis, over angle  $\varphi_A$  ( $A_2B_2 \rightarrow AB$ ). In the example shown the ligator atom A is characterized by  $\psi_A = \pi/2$ ,  $\theta_A = \pi/2$ , and  $\varphi_A = -\delta/2$ .

over an angle  $\varphi_A$ , leading to AB, which is the standard position of 4. From Figure 1, it is obvious that in this particular case  $\psi_A = \pi/2$  and  $\psi_B = 3\pi/2$ . A similar set of rotations can move a rigid chelate ligand to any other arbitrary position, and in general, it can be shown that

$$\cos \psi_A = (\cos \theta_A \sin \theta_B \cos (\varphi_A - \varphi_B) - \sin \theta_A \cos \theta_B) / \sin \delta \quad (19a)$$

$$\sin \psi_A = \sin \theta_B \sin (\varphi_B - \varphi_A) / \sin \delta \quad (19b)$$

$$\cos \psi_B = (\sin \theta_A \cos \theta_B \cos (\varphi_A - \varphi_B) - \cos \theta_A \sin \theta_B) / \sin \delta \quad (19c)$$

$$\sin \psi_B = \sin \theta_A \sin (\varphi_A - \varphi_B) / \sin \delta \quad (19d)$$

$$0 \leq \psi_A, \psi_B \leq 2\pi$$

These equations yield  $\psi_A$  and  $\psi_B$  in the interval  $[0, 2\pi]$  as functions of the angular coordinates of the ligator atoms and the bite angle  $\delta$ .

As for the interligand potential  $\mathcal{V}^{\text{cplng}}$ , an appropriate procedure must be introduced in order to generalize the discussion of the previous section (IIB). The most natural reference position for  $\mathcal{V}^{\text{cplng}}$  appears to be the situation described in 4, since it is characterized by a diagonal matrix in the  $\{|xz\rangle|yz\rangle\}$  basis. Indeed, from eq 11 and 17a one finds

$$\begin{array}{cc} \mathcal{V}^{\text{cplng}} & \begin{array}{c} |xz\rangle \\ |yz\rangle \end{array} \\ \begin{array}{c} \langle xz| \\ \langle yz| \end{array} & \begin{array}{cc} 2\pi_{\perp}^{AB} \cos^2(\delta/2) & 0 \\ 0 & -2\pi_{\perp}^{AB} \sin^2(\delta/2) \end{array} \end{array} \quad (20)$$

This interaction matrix is equivalent to the interaction of a pseudoligand X, which is located on the z axis, i.e. in the AOM reference position, and contributes only  $\pi$  interactions.

$$\begin{array}{cc} \pi_{xz}(X) = 2\pi_{\perp}^{AB} \cos^2(\delta/2) \\ \pi_{yz}(X) = -2\pi_{\perp}^{AB} \sin^2(\delta/2) & \sigma(X) = 0 \end{array} \quad (21)$$

The  $\pi_{xz}(X)$  parameter describes the  $\pi$  interaction along the bisector axis; the  $\pi_{yz}(X)$  parameter describes the  $\pi$  interaction

perpendicular to the bisector axis. We recall that no new parameters are involved since  $\pi_{\perp}^{AB}$  is defined as a function of  $\pi_{\perp}^A$  and  $\pi_{\perp}^B$  (see eq 10c). One should not think of X as a bridging ligand: it is formally introduced to mimic the nonadditive  $\pi$  contribution in the bidentate field. The angular dependence of the phase-coupling matrix is an exact copy of the angular dependence of the ligand field, exerted by this pseudoligand X. The  $(\theta, \varphi)$  coordinates of X are simply those of the perpendicular to the chelate plane.<sup>10</sup> The third coordinate,  $\psi_X$ , describes the orientation of the chelate bisector axis. The three coordinates can easily be found by requiring that the AOM rotation,<sup>9</sup>  $\mathcal{R}_z(\varphi_X)\mathcal{R}_y(\theta_X)\mathcal{R}_z(\psi_X)$ , which moves the pseudoligand X from the reference position  $(0, 0, 0)$  to the  $(\theta_X, \varphi_X, \psi_X)$  position, simultaneously carries the AB chelate from the standard position, represented in 4, to the general position  $(\theta_A, \varphi_A; \theta_B, \varphi_B)$ . As a result one obtains

$$\cos \theta_X = \sin (\varphi_B - \varphi_A) \sin \theta_A \sin \theta_B / \sin \delta \quad 0 \leq \theta_X \leq \pi \quad (22a)$$

$$\cos \varphi_X = (\sin \theta_A \cos \theta_B \sin \varphi_A - \cos \theta_A \sin \theta_B \sin \varphi_B) / (\sin \delta \sin \theta_X)$$

$$\sin \varphi_X = (\cos \theta_A \sin \theta_B \cos \varphi_B - \sin \theta_A \cos \theta_B \cos \varphi_A) / (\sin \delta \sin \theta_X) \quad 0 \leq \varphi_X \leq 2\pi \quad (22b)$$

$$\cos \psi_X = (\cos \theta_X \sin \theta_A \cos (\varphi_A - \varphi_X) + \cos \theta_X \sin \theta_B \cos (\varphi_B - \varphi_X) - \sin \theta_X (\cos \theta_A + \cos \theta_B)) / (2 \cos (\delta/2))$$

$$\sin \psi_X = (\sin \theta_A \sin (\varphi_A - \varphi_X) + \sin \theta_B \sin (\varphi_B - \varphi_X)) / (2 \cos (\delta/2)) \quad 0 \leq \psi_X \leq 2\pi \quad (22c)$$

### III. Applications

**A. Determination of the Bidentate Character.** So far our treatment of the Orgel effect was limited to the interaction of one frontier ligand orbital. However, identification of the dominant orbital interaction is not always straightforward. The  $d\pi$  orbitals are generally considered to be situated between one filled  $\pi$  orbital (HOMO) and one empty  $\pi^*$  orbital (LUMO), which in principle can both contribute to the ligand field. If both interactions are of similar importance, the overall  $\pi$  contributions in the *additive* field formalism tend to fade, since the respective  $\pi$  parameters have opposite sign. In consequence, strong orbital interactions do not always show up in the AOM parameters.

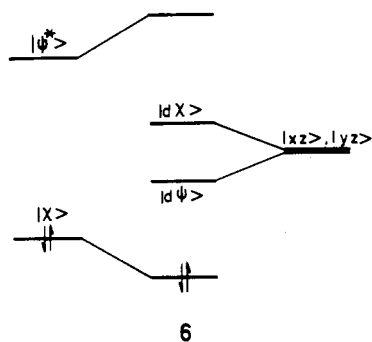
Quite to the contrary, the synergism between  $\pi$ -donor and  $\pi$ -acceptor interactions may lead to a *more pronounced Orgel effect*. Indeed, it is frequently observed that HOMO and LUMO of the conjugated bidentate adopt alternate phases of the outer orbitals. As a result, the interligand part of the potential is reinforced since the change of sign from  $\pi$ -donor to  $\pi$ -acceptor parameters is offset by the phase alternation from ligand HOMO to ligand HUMO. Hence, the  $d\pi$ -orbital polarization *increases* as compared to the effect of HOMO and LUMO interactions taken separately. As an example, a  $\chi$ -type-donor orbital destabilizes the  $|d\chi\rangle$  combination (see eq 4) while a  $\psi$ -type-acceptor orbital simultaneously stabilizes the complementary combination  $|d\psi\rangle$ , as illustrated in 6. In conclusion, simple Hückel theory often leads to an unequivocal prediction of the sign of the splitting, even if it is not clear whether donor or acceptor interactions are predominant.

In the case of a four-membered chelating bridge,  $\pi$  conjugation resembles the  $\pi$  system in butadiene, i.e. the filled frontier orbital is out of phase coupled, and the lowest acceptor orbital is of the  $\psi$  type,<sup>11</sup> exactly as sketched in 6. Typical ligands are  $\alpha$ -diimine

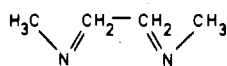
(9) Schäffer, C. E. XIIIth International Conference on Coordination Chemistry, IUPAC; Butterworths: London, 1970; p 361.

(10) Obviously X can be placed on either side of the chelate plane. Since the holohedron symmetry concept<sup>9</sup> also applies to the  $\mathcal{V}^{\text{cplng}}$  matrix, both positions will yield exactly the same result, and the formal introduction of a third ligand will not lower the  $C_{2v}$  (or  $C_2$ ) symmetry of the  $M(A-A)$  (or  $M(A-B)$ ) unit. The positional choice made in eq 20 and 21 is the following: for an observer in X the rotation from A to B over the bidentate angle  $\delta$  will appear counterclockwise. This convention is also used in the general expressions of eq 22.

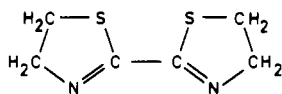
(11) Ito, T.; Tanaka, N.; Hanazaki, I.; Nagakura, S. *Bull. Chem. Soc. Jpn.* **1968**, *41*, 365.



ligands such as glyoxal bis(*N*-methylimine)<sup>12</sup> (gmi) (7) or 2,2'-bi-2-thiazoline<sup>13</sup> (bt) (8).



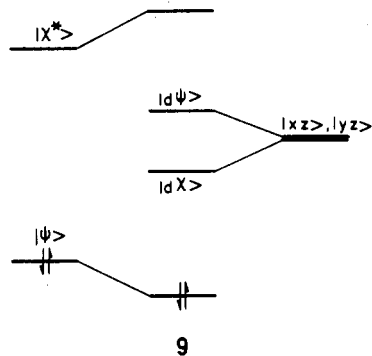
gmi 7



bt 8

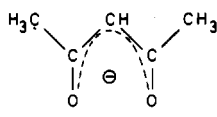
More complex homologues that still contain the  $\alpha$ -diimine moiety not necessarily will show the same splitting sign. Indeed, orbital calculations on the 1,10-phenanthroline (phen) ligand, coordinated to divalent iron, indicate that the chelate contains two almost degenerate acceptor levels of both  $\psi^*$  and  $\chi^*$  character.<sup>14</sup> This is confirmed by the observation of a complex band system in the visible spectrum of the  $\text{Fe}(\text{phen})_3^{2+}$  ion, covering  $d\pi \rightarrow \psi^*$  and  $d\pi \rightarrow \chi^*$  charge-transfer absorptions. Clearly, in this case the sign of the Orgel effect cannot be inferred from simple Hückel theory.

Five-membered conjugated chains copy the  $\pi$  system of the pentadiene anion. In this case the symmetries of HOMO and LUMO are reversed as compared to the butadiene template (9).

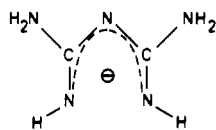


9

Typical examples are the  $\beta$ -diketonate ligands<sup>15,16</sup> such as acetylacetonate (acac) (10),  $\beta$ -diiminate ligands<sup>17</sup> such as biguanidate (bgd) (11), or mixed oxygen-nitrogen donors.



acac 10



bgd 11

**B. Bis Chelate Complexes.** To illustrate the technique of matrix rotation we will elaborate the example of a bis chelate complex with four identical coordinating atoms at the vertices of a regular tetrahedron (see Figure 2). The bite angle  $\delta$  adopts the tetrahedral value of  $109.47^\circ$ . Angular coordinates of the ligators and the two

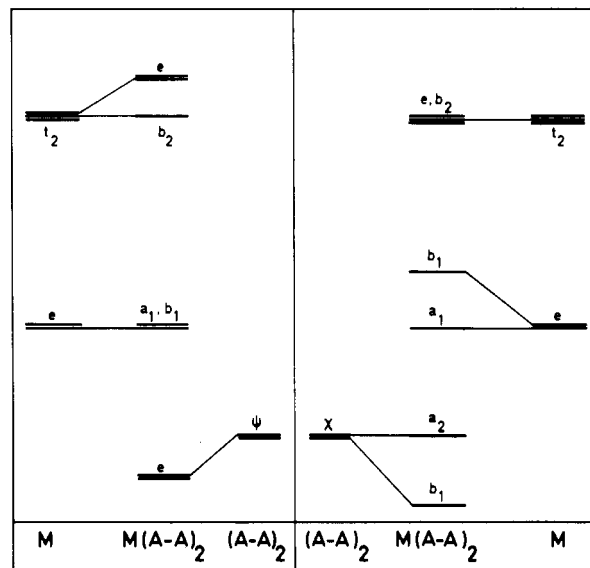
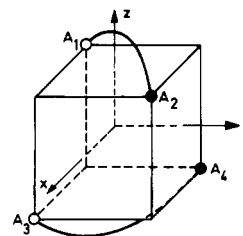


Figure 2. Orbital energy diagram for a pseudotetrahedral bis chelate complex, under a  $\psi$ - or a  $\chi$ -type bidentate field. Corresponding d-orbital energy expressions are listed in Table II.  $\pi_{||}$  interactions were considered negligible. The molecular symmetry group is  $D_{2d}$ .

Table I. Model Input Parameters for a Pseudotetrahedral Bis Chelate, Shown in Figure 2

ligands	angular coord			model parameters		
	$\theta$	$\varphi$	$\psi$	$\sigma$	$\pi_{xz}$	$\pi_{yz}$
$A_1$	54.74	225.0	180.0	$\sigma$	$\pi_{  }$	$\pi_{\perp}$
$A_2$	54.74	45.0	180.0	$\sigma$	$\pi_{  }$	$\pi_{\perp}$
$A_3$	125.26	315.0	0.0	$\sigma$	$\pi_{  }$	$\pi_{\perp}$
$A_4$	125.26	135.0	0.0	$\sigma$	$\pi_{  }$	$\pi_{\perp}$
$X_1$	90.0	135.0	180.0	0.0	$2/3\pi_{\perp}$	$-4/3\pi_{\perp}$
$X_2$	90.0	45.0	0.0	0.0	$2/3\pi_{\perp}$	$-4/3\pi_{\perp}$

Table II. Energy Expressions for the d Orbitals in a Pseudotetrahedral Bis Chelate Complex, Shown in Figure 2 (See Also Table I)

	bidentate field	
	$\psi$ -type	$\chi$ -type
$ xz\rangle$	$4/3\sigma + 2/9\pi_{  } + 4/3\pi_{\perp}$	$4/3\sigma + 2/9\pi_{  }$
$ yz\rangle$	$4/3\sigma + 2/9\pi_{  } + 4/3\pi_{\perp}$	$4/3\sigma + 2/9\pi_{  }$
$ xy\rangle$	$4/3\sigma + 8/9\pi_{  }$	$4/3\sigma + 8/9\pi_{  }$
$ z^2\rangle$	$8/3\pi_{  }$	$8/3\pi_{  }$
$ x^2 - y^2\rangle$	0.0	$16/3\pi_{\perp}$

pseudoligands, calculated according to eq 19 and 22 are collected in Table I. Also tabulated are the AOM parameters for each ligand. The pseudoligand  $\pi$  parameters were obtained from eq 21. The resulting interaction matrix, constructed on the basis of these input data, was found to be diagonal for both  $\psi$ - and  $\chi$ -type ligand orbitals. The relevant orbital energies are listed in Table II. Figure 2 resumes the corresponding orbital interaction diagrams. As can be seen from the figure the calculated d-orbital energy splittings reflect the symmetry lowering of the tetrahedral field, uniquely due to the bonding coupling in the bidentates.<sup>18</sup>

- (12) Blomquist, J.; Nordén, B.; Sundbom, M. *Theor. Chim. Acta* **1973**, *28*, 313.  
 (13) Krug, W. P.; Demas, J. N. *J. Am. Chem. Soc.* **1979**, *101*, 4394.  
 (14) Ito, T.; Tanaka, N.; Hanazaki, J.; Nagakura, S. *Bull. Chem. Soc. Jpn.* **1969**, *42*, 702.  
 (15) Barnum, D. W. *J. Inorg. Nucl. Chem.* **1961**, *21*, 221.  
 (16) Fackler, J. P.; Cotton, F. A.; Barnum, D. W. *Inorg. Chem.* **1963**, *2*, 97.  
 (17) Moucharfieh, N. C.; Eller, P. G.; Bertrand, J. A.; Royer, D. *J. Inorg. Chem.* **1978**, *17*, 1220.

- (18) Lin, W. C.; Orgel, L. E. *Mol. Phys.* **1963**, *7*, 131.

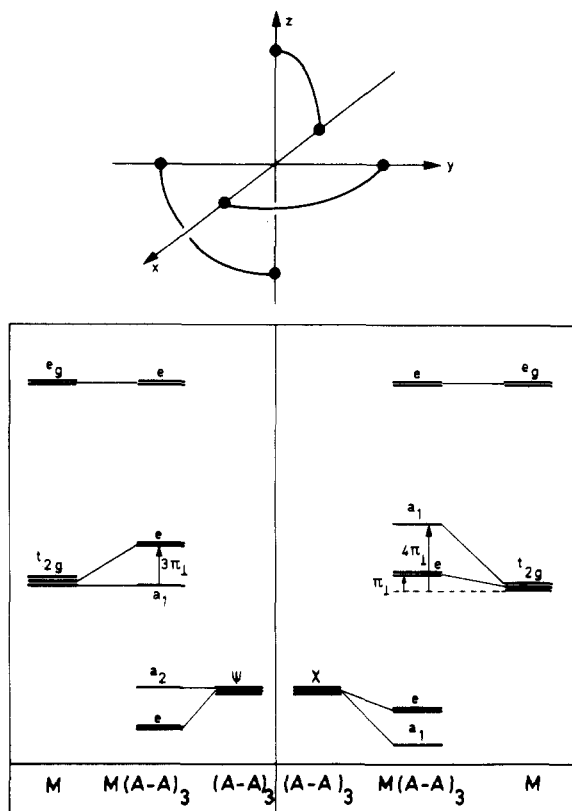
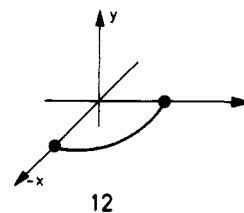


**Figure 3.** Orbital energy diagram for a pseudooctahedral tris chelate complex, under a  $\psi$ - or a  $\chi$ -type bidentate field.  $\pi$  interactions only involve the  $t_{2g}$  orbitals (cf. eq 24). The molecular symmetry group is  $D_3$ .

Although several pseudotetrahedral bis chelate complexes are known, virtually no accurate spectroscopic measurements are available.<sup>19</sup> On the other hand, spectral characterization of the electronic structure in square-planar bis chelate complexes has been remarkably successful. Especially Schiff base complexes of divalent cobaltum have been extensively studied.<sup>20</sup> Characteristic parameters of the present model such as sign and magnitude of the Orgel effect and the eigenvector directions have been determined unambiguously. A detailed discussion of these results will be the aim of a subsequent paper.<sup>8</sup>

**C. Tris Chelate Complexes.** Rather than treating the problem of tris chelation in full generality, we choose to focus on a simple example that illustrates the essential features of the Orgel effect, without going through extensive matrix rotations. In what follows, ligand atoms will be assumed to form a regular octahedron ( $\delta = \pi/2$ ); bidentates are taken to be symmetrical, and  $\pi_{\parallel}$  interactions are neglected. Coordinate axes are aligned with the octahedral frame as shown in Figure 3.

The  $\pi_{\perp}$ -interaction matrix can now be constructed on the basis of the simple principles, used in section IIA. First, we note that the contribution of the bidentate in the  $xy$  plane is already available in eq 3 and 4. The bidentate field of the other two chelating groups can immediately be obtained from these equations, by carrying out the appropriate substitutions of  $d\pi$  orbitals. For instance, if we redraw the bidentate in the  $xz$  plane (Figure 3) as in 12 and compare this with the corresponding sketch for a bidentate in the  $xy$  plane (1 and 2), it is recognized at once that the role of the



$|xz\rangle$  and  $|yz\rangle$  orbitals in section IIA is now taken over by  $-|xy\rangle$  and  $|yz\rangle$  orbitals. Hence, it is sufficient to rewrite the interaction matrices in eq 3, 4 in the new orbital basis, yielding, e.g., for a  $\psi$ -type ligand

$$\begin{array}{ccc|ccc} \mathcal{V}(\psi) & -|xy\rangle & |yz\rangle & & \mathcal{V}(\psi) & |xz\rangle & |yz\rangle \\ -\langle xy| & \pi_{\perp} & \pi_{\perp} & \text{or} & \langle xy| & \pi_{\perp} & -\pi_{\perp} \\ \langle yz| & \pi_{\perp} & \pi_{\perp} & & \langle yz| & -\pi_{\perp} & \pi_{\perp} \end{array} \quad (23)$$

Summing the contributions of the three bidentate ligands, one finally arrives at the total  $\pi_{\perp}$ -interaction matrices given in (24).

$$\begin{array}{ccc|ccc} \mathcal{V}(\psi) & |xz\rangle & |yz\rangle & |xy\rangle & \mathcal{V}(\chi) & |xz\rangle & |yz\rangle & |xy\rangle \\ \langle xz| & 2\pi_{\perp} & \pi_{\perp} & \pi_{\perp} & \langle xz| & 2\pi_{\perp} & -\pi_{\perp} & -\pi_{\perp} \\ \langle yz| & \pi_{\perp} & 2\pi_{\perp} & -\pi_{\perp} & \langle yz| & -\pi_{\perp} & 2\pi_{\perp} & \pi_{\perp} \\ \langle xy| & \pi_{\perp} & -\pi_{\perp} & 2\pi_{\perp} & \langle xy| & -\pi_{\perp} & \pi_{\perp} & 2\pi_{\perp} \end{array} \quad (24)$$

The eigenvalue levels are represented in Figure 3. The corresponding eigenorbitals are the well-known  $t_{2g}$  functions, quantized along the trigonal molecular axis.<sup>21</sup> Again one observes a strikingly different Orgel effect, depending on the type of frontier orbital. While symmetry can explain the sign of the trigonal splitting in the case of a  $\psi$ -type interaction, the  $t_{2g}$ -orbital order in a  $\chi$ -type bidentate field could not have been deduced from symmetry alone. If  $\mathcal{V}(\psi)$  and  $\mathcal{V}(\chi)$  are averaged, the  $t_{2g}$  threefold degeneracy is restored. Hence, the additive angular-overlap model of the first coordination sphere (even in its nonlinear ligand version with  $\pi_{\parallel} \neq \pi_{\perp}$ ) was unable to account for the large trigonal splittings of the  $d\pi$  orbitals in quasi-octahedral tris chelates.

Recent circular and linear dichroism measurements of d-d transitions in tris-chelated Co(III) complexes, involving  $\pi$ -conjugated bidentates, indeed reveal the presence of large trigonal fields.<sup>22,23</sup> In contrast, saturated tris chelates such as tris(ethylenediamine) complexes usually give rise to very weak trigonal perturbations.

Furthermore, the  $t_{2g}$ -orbital order in the unsaturated tris-chelated complexes,  $\text{Co}(\text{acac})_3$  and  $\text{Co}(\text{bgd})_3$  (see 10 and 11) is found to correspond to the order that is characteristic of a  $\psi$ -type donor orbital on the ligand<sup>17</sup> (Figure 3). This is indeed in agreement with the expectations from simple MO theory, set forth in section IIIA (9).

Anisotropic ligation, due to coupled bonding, can also be observed in the metal-to-ligand charge-transfer bands of tris(diimine) complexes of Fe(II), Ru(II), and Os(II).<sup>24</sup> The intensity distribution among the different dipole-allowed transitions can be understood on the basis of a typical Orgel effect in the bidentate field of a  $\psi$ -acceptor orbital. Again, this assignment follows the qualitative predictions in section IIIA (6).

**Acknowledgment.** The authors gratefully acknowledge financial support from the Belgian Government (Programmatie van het Wetenschapsbeleid). A.C. is indebted to the Belgian Science Foundation (NFWO).

- (19) Daul, C.; Schläpfer, C. W.; Goursot, A.; Pénigault, E.; Weber, J. *Chem. Phys. Lett.* **1981**, *78*, 304.  
 (20) Daul, C.; Schläpfer, C. W.; von Zelewsky, A. *Struct. Bonding (Berlin)* **1979**, *36*, 129.

- (21) Liehr, A. D. *J. Phys. Chem.* **1964**, *68*, 665.  
 (22) Peacock, R. D.; Stewart, B. *Coord. Chem. Rev.* **1982**, *46*, 129.  
 (23) Peacock, R. D. *J. Chem. Soc., Dalton Trans.* **1983**, 291.  
 (24) Ceulemans, A.; Vanquickenborne, L. G. *J. Am. Chem. Soc.* **1981**, *103*, 2238.